

Einstein-Podolsky-Rosen paradox in a hybrid bipartite system

MICHAŁ DĄBROWSKI¹, MICHAŁ PARNIAK^{1,*}, AND WOJCIECH WASILEWSKI¹

¹Institute of Experimental Physics, Faculty of Physics, University of Warsaw, Pasteura 5, 02-093 Warsaw, Poland

*Corresponding author: michal.parniak@fuw.edu.pl

Compiled February 20, 2017

Entanglement of light and matter is an essential resource for effective quantum engineering. In particular, collective states of atomic ensembles are robust against decoherence while preserving the possibility of strong interaction with quantum states of light. While previous approaches to continuous-variable quantum interfaces relied on quadratures of light, here we present an approach based on spatial structure of light-atom entanglement. We create and characterize a 12-dimensional entangled state exhibiting quantum correlations between a photon and an atomic ensemble in position and momentum bases. This state allows us to demonstrate the original Einstein-Podolsky-Rosen (EPR) paradox with two different entities, with an unprecedented delay time of 6 μ s between generation of entanglement and detection of the atomic state. © 2016 Optical Society of America

OCIS codes: (020.0020) Quantum optics; (270.5585) Quantum information and processing; (230.1040) Atomic and molecular physics.

<http://dx.doi.org/10.1364/optica.XX.XXXXXX>

With the rapid development of spatially-resolving single-photon detectors, spatially structured multidimensional entangled states start to play a key role in modern quantum science. In particular, they find extensive applications in emerging fields such as quantum imaging [1, 2], holography [3], computation [4] or quantum-enhanced metrology [5]. Moreover, spatially-multiplexed schemes hold a promise to increase the capacity of quantum channels, essential for quantum key distribution [6]. An appealing perspective is to apply these ideas to light-atom interfaces, that are capable of storing and processing continuous-variable (CV) entanglement [7], critical for novel quantum cryptography [8], computation [9] and imaging [10] schemes.

The foundations for these modern ideas have been laid down by Einstein, Podolsky and Rosen [11] in their famous *Gedankenexperiment* that was designed to prove the quantum theory is incomplete. They considered an entangled state of two particles with perfectly correlated positions and anti-correlated momenta. Such a state exhibits an apparent paradox, namely the product of conditional variances of positions and momenta violate the

Heisenberg inequality $\Delta x \Delta p_x \geq \hbar/2$, suggesting the failure of local realism. In contrast to what EPR predicted, an experiment conducted with spin-entangled states [12] demonstrated non-local features of quantum mechanics. Later came the demonstrations of the EPR paradox with CV entangled systems, namely quadratures of light in optical parametric oscillators [7, 13, 14], four-wave mixing [10] and recently spin-quadratures of a degenerate quantum gas [15]. Original EPR proposal with true positions and momenta was realized with photons obtained in spontaneous parametric down-conversion [16–19] and spontaneous four-wave mixing [20], initiating the trend to explore spatial structure of entangled states of light.

Here we generate a hybrid bipartite entangled state of a photon and an atomic spin-wave excitation and demonstrate the EPR paradox with position and momenta of two different entities. We verify the entanglement by measuring the coincidence patterns corresponding to modulus-squared spatial wavefunctions of the state. By studying temporal evolution and decoherence we find that the EPR entanglement may be stored for several microseconds, which greatly outstrips the previous approach based on quadratures of squeezed light and a slow-light medium [10]. Spatial entanglement gives a promise to enhance the capacity of quantum memories [21–24] and repeater protocols derived from the Duan-Lukin-Cirac-Zoller (DLCZ) scheme [25].

The hybrid entangled state is prepared via a two-mode squeezing Raman interaction, depicted in Fig. 1, which creates pairs of Stokes photons and spin-wave excitations with anti-correlated momenta. A single spin-wave excitation with momentum $\mathbf{P} = (P_x, P_y)$ is defined as the state of N atoms created by acting with the $\hat{b}_{\mathbf{p}}^{\dagger}$ operator on the spin-wave vacuum:

$$\hat{b}_{\mathbf{p}}^{\dagger}|0\rangle = \sum_{j=1}^N \exp\left(\frac{i}{\hbar}\mathbf{P}\cdot\mathbf{R}_j\right) |g_1 \dots h_j \dots g_N\rangle, \quad (1)$$

where \mathbf{R}_j is the position of j -th atom and $|g\rangle, |h\rangle$ are the two metastable states defined in Fig. 1(d). For low probability amplitude ϵ of entangled pair generation ($\epsilon \ll 1$) we approximate the spatial structure of the momentum anti-correlated squeezed state by $|00\rangle + \int d\mathbf{p} d\mathbf{P} \Psi(\mathbf{p}, \mathbf{P}) \hat{a}_{\mathbf{p}}^{\dagger} \hat{b}_{\mathbf{P}}^{\dagger} |00\rangle$, where $\hat{a}_{\mathbf{p}}^{\dagger}$ is the creation operator for photon with momentum $\mathbf{p} = (p_x, p_y)$, with the unnormalized Gaussian-shaped wavefunction [18]:

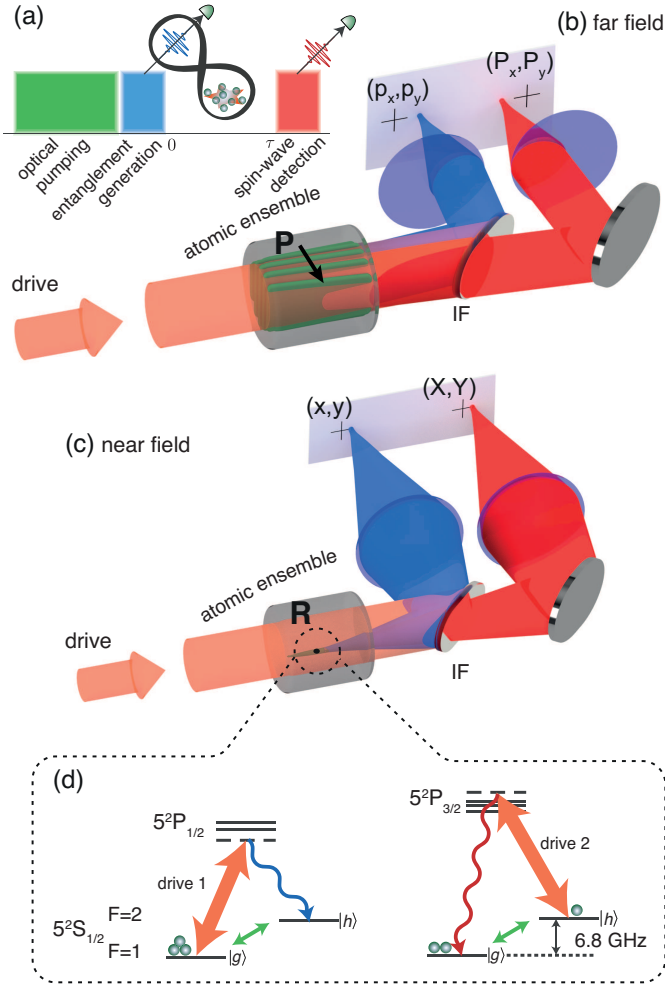


Fig. 1. (a) The pulse sequence used to generate and then characterize the hybrid EPR entangled state. (b) The setup projecting the far field of the atomic ensemble onto the camera, enabling measurement in the momentum basis, corresponding to spin-wave-shaped collective atomic excitation. (c) An analogous setup imaging the atomic ensemble onto the detector plane, which enables measurement of positions in the atomic ensemble from which the photons are emitted. (d) The relevant atomic level scheme of rubidium-87. Since the two driving lasers operate at different rubidium lines, the photons can be separated with an interference filter (IF).

$$\tilde{\Psi}(\mathbf{p}, \mathbf{P}) = \epsilon \frac{\sigma_- \sigma_+}{\pi} \exp\left(-\sigma_+^2 \frac{|\mathbf{p} + \mathbf{P}|^2}{4\hbar^2} - \sigma_-^2 \frac{|\mathbf{p} - \mathbf{P}|^2}{4\hbar^2}\right), \quad (2)$$

in a complete analogy to the biphoton wavefunction. By Fourier-transforming the wavefunction we obtain a position representation of the state [17, 18]:

$$\Psi(\mathbf{r}, \mathbf{R}) = \epsilon \frac{1}{\pi\sigma_- \sigma_+} \exp\left(-\frac{|\mathbf{r} - \mathbf{R}|^2}{4\sigma_-^2} - \frac{|\mathbf{r} + \mathbf{R}|^2}{4\sigma_+^2}\right) \quad (3)$$

and find that the position of photons $\mathbf{r} = (x, y)$ and spin-wave excitations $\mathbf{R} = (X, Y)$ are correlated, where $\sigma_{\pm}^2 = \langle \Delta^2 |\mathbf{r} \pm \mathbf{R}| \rangle$.

To witness the EPR paradox, we consider the variances of composite variables, namely sum of momenta ($p_x + P_x$) and difference of positions ($x - X$) from the wavefunctions definitions given by Eqs. (2) and (3), respectively. As derived by Reid

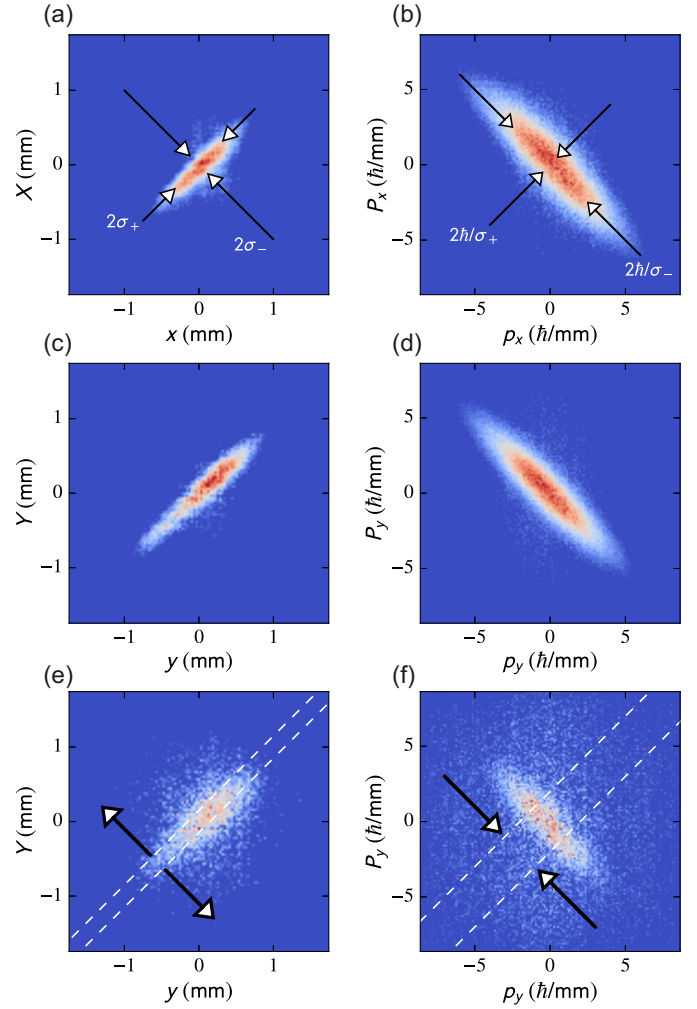


Fig. 2. Background-subtracted coincidence maps in positions [(a), (c)] and momenta [(b), (d)] for x [(a), (b)] and y dimensions [(c), (d)] for the shortest delay time $\tau = 250$ ns, integrated over the perpendicular dimension. Correlations in positions and anti-correlations in momenta are clearly visible. [(e), (f)] Results precisely corresponding to the ones presented in [(c), (d)], but for a delay time of $\tau = 3 \mu\text{s}$.

[26, 27], the EPR paradox occurs if the following inequality is satisfied:

$$\langle \Delta^2(x - X) \rangle \langle \Delta^2(p_x + P_x) \rangle < \hbar^2/4. \quad (4)$$

However, if the above product is larger than $\hbar^2/4$, the bipartite state may still be entangled. The condition for inseparability is given by $\langle \Delta^2(x - X) \rangle \langle \Delta^2(p_x + P_x) \rangle < \hbar^2$, as proved by Mancini *et al.* [28]. Therefore, we may distinguish three different regimes: the classical separable regime, the EPR paradox regime, and the intermediate regime where the correlations, although of quantum origin, may not be strong enough to demonstrate the EPR paradox but only inseparability of the state.

We now consider the material spin-wave component of the entangled state. While the photon is sent through a free-space channel at a long distance, decoherence of the spin-wave excitation occurs. Through decoherence, a spin wave is lost and the atomic state returns to the spin-wave vacuum. The rate of this transition is given by $D|\mathbf{P}|^2/\hbar^2$, where D is the diffusion coefficient of atoms. As a consequence, the wavefunction from

Eq. (2) is multiplied by a factor of $\exp(-D|\mathbf{P}|^2\tau/\hbar^2)$ for delay time τ , resulting in a drop of the number of entangled pairs (see Section S3 of Supplement 1 for derivation). Additionally, the position and momentum variances are changed so that the dimension of entanglement [17], defined for delay time $\tau = 0$ as $D = (\sigma_+/\sigma_-)^2$ drops. Simultaneously the product of variances, essential to witness the EPR paradox, initially rises linearly in time as $\langle\Delta^2|\mathbf{r} - \mathbf{R}\rangle\langle\Delta^2|\mathbf{p} + \mathbf{P}\rangle \approx \hbar^2(\sigma_-^2 + D\tau)/\sigma_+^2$. As far as the maximum dimension of entanglement is concerned, we consider the initial σ_{\pm}^2 variances. Due to decoherence during the generation and detection operations, which take a finite total amount of time T to perform, the initial σ_-^2 variance is lower-bounded by roughly the mean-squared atomic displacement DT . On the other hand, the σ_+^2 variance is upper-bounded by the squared waist radius of the driving beam.

In the experiment we use a 10-cm-long quantum memory vacuum cell containing $N \approx 10^{12}$ warm (75 °C) rubidium-87 atoms and krypton at 1 Torr as a buffer gas to make the atomic motion diffusive. The entanglement is generated by the driving beam illuminating the ensemble of atoms previously prepared in the $|g\rangle$ state ($5^2S_{1/2}$, $F = 1$) by optical pumping, which constitutes a spin-wave vacuum. We conduct the experiment in the spontaneous regime with 0.05 pairs on average generated per single spatial mode in each realization of the experiment, with no amplification due to build-up of spin-waves. To detect the atomic spin-wave stored inside atomic ensemble we use stimulated Raman interaction. By sending driving pulse from another laser after an arbitrary delay time τ , as seen in Fig. 1(d), we perform an on-demand conversion of a single atomic spin-wave excitation with momentum \mathbf{P} to an anti-Stokes photon with momentum determined by the phase-matching condition [29]. All scattered photons are first separated from the driving lasers light and stray fluorescence using a three-stage filtering system and finally registered using state-of-the-art single-photon sensitive camera with image intensifier (I-sCMOS) [3], situated in the near or the far field which corresponds to the measurement of (\mathbf{r}, \mathbf{R}) or (\mathbf{p}, \mathbf{P}) observables, respectively. These two imaging configurations are selectable using flip mirrors (see Section S1 of Supplement 1 for more experimental details).

In Fig. 2 we present measured bidimensional coincidence maps corresponding to the modulus-squared wavefunction integrated over the perpendicular direction. We consider all pairs of registered photons from the two regions of interest of the camera, mark their positions in the joint statistics map and at the end subtract the background of accidental coincidences (see Section S2 of Supplement 1 for details on how the data is processed). The coincidence maps clearly demonstrate correlations in positions and at the same time anti-correlations in momenta, as expected from the EPR state. After a certain delay time, the expected effect of diffusional decoherence, apart from the drop of signal-to-noise ratio, is expansion, or blurring of the coincidence pattern in the position space. Simultaneously, we observe the shrinkage of the far-field pattern, corresponding to the decay of high momentum spin-waves, in accordance with the Fourier-transform principle. In turn, the dimension of entanglement D decreases.

To quantify the entanglement of the generated EPR state we use the criterion given by Eq. (4). Similarly as in Fig. 2, we consider the distributions of all registered pairs and subtract the accidental coincidences. The results presented in Fig. 3 are narrow two-dimensional peaks at zero coordinates for sum of momenta and difference of positions (see Section S2 of Supplement

1 for cross sections). The width of the peak allows us to estimate the degree of violation of EPR criterion [Eq. (4)] as well as the amount of entanglement in the system. We find slightly different σ_{\pm}^2 variances for the x and y -dimensions, which is due to particular arrangement of the experimental setup. Consequently, stronger degree of entanglement is witnessed in the y -dimension where we observe the EPR paradox until 9 μs delay time. For the full two-dimensional coincidence distributions, we average the variances of two-dimensional variables (\mathbf{r}, \mathbf{R}) and (\mathbf{p}, \mathbf{P}) for the total position and momentum [30]. Finally, for the shortest delay time of $\tau = 250$ ns we obtain the results presented in

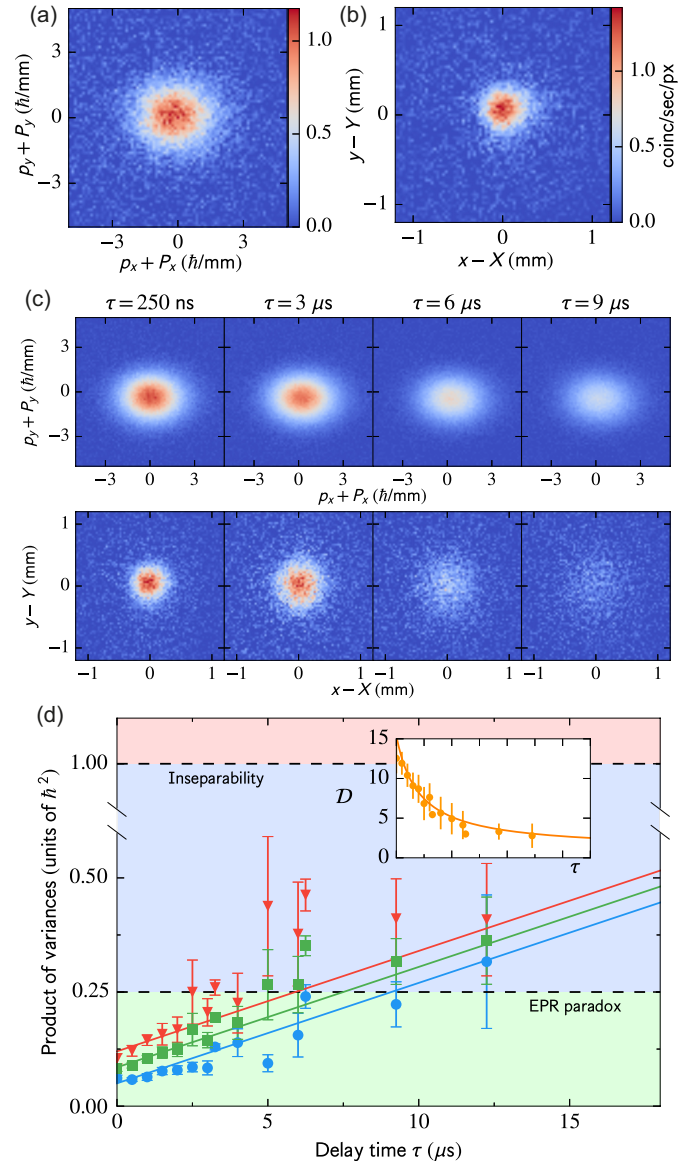


Fig. 3. Demonstration of the EPR paradox. [(a), (b)] Number of coincidences in terms of composite variables for the shortest delay time of $\tau = 250$ ns. (c) The same distributions portrayed for a set of different delay times. (d) The product of variances. Solid lines correspond to the expected decay of entanglement due to atomic diffusion for x -dimension (red triangles), y -dimension (blue circles) and calculated averages for the full transverse image [30] (green squares). Inset shows the corresponding dimension of entanglement D .

Table 1. Values of variances and their products for $\tau = 250$ ns.

Variances	Experimental values	Product
$\langle \Delta^2(x - X) \rangle$	0.040(4) mm ²	0.10(1) \hbar^2
$\langle \Delta^2(p_x + P_x) \rangle$	2.6(1) \hbar^2 /mm ²	
$\langle \Delta^2(y - Y) \rangle$	0.040(4) mm ²	0.061(6) \hbar^2
$\langle \Delta^2(p_y + P_y) \rangle$	1.50(4) \hbar^2 /mm ²	
$\langle \Delta^2 \mathbf{r} - \mathbf{R} \rangle$	0.040(3) mm ²	0.082(6) \hbar^2
$\langle \Delta^2 \mathbf{p} + \mathbf{P} \rangle$	2.05(6) \hbar^2 /mm ²	

Table 1 and calculate the dimension of entanglement $\mathcal{D} = 12.2 \pm 0.9$. Values and uncertainties are inferred from Gaussian fittings to experimental coincidence maps in Figs. 3(a) and 3(b).

The model of decoherence with predicted linear rise of the product of variances fits well to our experimental data, as presented in Fig. 3(d) (see Section S3 of Supplement 1 for derivation). In particular, after 6 μ s delay time the dimension of entanglement \mathcal{D} drops so that we are no longer able to certify the EPR paradox, although the joint state is still inseparable. Notably, even though the net storage efficiency drops rapidly with time as high-momentum spin-waves are lost, we observe that our hybrid bipartite system is still non-classically correlated in positions and momenta.

In conclusion, we demonstrate generation and characterization of a hybrid entangled state of light and matter exhibiting EPR correlations in real space of continuous position-momentum variables, as in the original EPR proposal. As far as the EPR entanglement is concerned, our approach turns out to be by far more robust than the only hitherto performed experiment where time-delayed EPR correlations were demonstrated [10]. We achieve two orders of magnitude longer delay time using quantum memory setup and significantly stronger violation of EPR inequality [Eq. (4)], with product of variances 3 times below the EPR bound for the full two-dimensional coincidence distribution. Our discussion of contributing experimental factors gives prospects to further increase the dimension of entanglement.

The spatially-multimode structure of CV entanglement we generate is essential in terms of quantum information processing and communication, in particular it may provide significant enhancement for the DLCZ protocol [25] or improvement of photon sources [29]. Temporally-multimode solutions [31, 32] available in very similar systems ask for the connection with spatial multiplexing and polarization degree of freedom to enable demonstrations of multimode hyperentanglement [24, 33] or EPR entanglement with more than two parties [34, 35]. The possibility to manipulate the stored atomic state opens new avenues in the vivid topic of EPR-steering [36], thus providing ways to perform novel tests of the quantum theory.

Funding. National Science Centre (Poland) Grants No. 2011/03/D/ST2/01941, 2015/19/N/ST2/01671 and Polish Ministry of Science and Higher Education “Diamantowy Grant” Project No. DI2013 011943.

Acknowledgments. We acknowledge inspiring discussions with K. Banaszek and R. Łapkiewicz, as well as proofreading of the manuscript by R. Chrapkiewicz, M. Jachura and M. Lipka.

See Supplement 1 for supporting content.

REFERENCES

- R. S. Bennink, S. J. Bentley, R. W. Boyd, and J. C. Howell, Phys. Rev. Lett. **92**, 033601 (2004).
- G. B. Lemos, V. Borish, G. D. Cole, S. Ramelow, R. Lapkiewicz, and A. Zeilinger, Nature **512**, 409 (2014).
- R. Chrapkiewicz, M. Jachura, K. Banaszek, and W. Wasilewski, Nat. Photonics **10**, 576 (2016).
- D. S. Tasca, R. M. Gomes, F. Toscano, P. H. Souto Ribeiro, and S. P. Walborn, Phys. Rev. A **83**, 052325 (2011).
- M. Jachura, R. Chrapkiewicz, R. Demkowicz-Dobrzański, W. Wasilewski, and K. Banaszek, Nat. Commun. **7**, 11411 (2016).
- S. P. Walborn, D. S. Lemelle, M. P. Almeida, and P. H. S. Ribeiro, Phys. Rev. Lett. **96**, 090501 (2006).
- K. Jensen, W. Wasilewski, H. Krauter, T. Fernholz, B. M. Nielsen, M. Owari, M. B. Plenio, A. Serafini, M. M. Wolf, and E. S. Polzik, Nat. Phys. **7**, 13 (2010).
- S. A. Goorden, M. Horstmann, A. P. Mosk, B. Škorić, and P. W. H. Pinkse, Optica **1**, 421 (2014).
- P. C. Humphreys, W. S. Kolthammer, J. Nunn, M. Barbieri, A. Datta, and I. A. Walmsley, Phys. Rev. Lett. **113**, 130502 (2014).
- A. M. Marino, R. C. Pooser, V. Boyer, and P. D. Lett, Nature **457**, 859 (2009).
- A. Einstein, B. Podolsky, and N. Rosen, Phys. Rev. **47**, 777 (1935).
- S. J. Freedman and J. F. Clauser, Phys. Rev. Lett. **28**, 938 (1972).
- Z. Y. Ou, S. F. Pereira, H. J. Kimble, and K. C. Peng, Phys. Rev. Lett. **68**, 3663 (1992).
- N. Takei, N. Lee, D. Moriyama, J. S. Neergaard-Nielsen, and A. Furusawa, Phys. Rev. A **74**, 060101 (2006).
- J. Peise, I. Kruse, K. Lange, B. Lücke, L. Pezzè, J. Arlt, W. Ertmer, K. Hammerer, L. Santos, A. Smerzi, and C. Klempt, Nat. Commun. **6**, 8984 (2015).
- J. C. Howell, R. S. Bennink, S. J. Bentley, and R. W. Boyd, Phys. Rev. Lett. **92**, 210403 (2004).
- M. P. Edgar, D. S. Tasca, F. Izdebski, R. E. Warburton, J. Leach, M. Agnew, G. S. Buller, R. W. Boyd, and M. J. Padgett, Nat. Commun. **3**, 984 (2012).
- P.-A. Moreau, F. Devaux, and E. Lantz, Phys. Rev. Lett. **113**, 160401 (2014).
- J. Schneeloch, P. B. Dixon, G. A. Howland, C. J. Broadbent, and J. C. Howell, Phys. Rev. Lett. **110**, 130407 (2013).
- J.-C. Lee, K.-K. Park, T.-M. Zhao, and Y.-H. Kim, Phys. Rev. Lett. **117**, 250501 (2016).
- H.-N. Dai, H. Zhang, S.-J. Yang, T.-M. Zhao, J. Rui, Y.-J. Deng, L. Li, N.-L. Liu, S. Chen, X.-H. Bao, X.-M. Jin, B. Zhao, and J.-W. Pan, Phys. Rev. Lett. **108**, 210501 (2012).
- S.-Y. Lan, A. G. Radnaev, O. A. Collins, D. N. Matsukevich, T. A. B. Kennedy, and A. Kuzmich, Opt. Express **17**, 13639 (2009).
- A. Nicolas, L. Veissier, L. Giner, E. Giacobino, D. Maxein, and J. Laurat, Nat. Photon. **8**, 234 (2014).
- W. Zhang, D.-S. Ding, M.-X. Dong, S. Shi, K. Wang, S.-L. Liu, Y. Li, Z.-Y. Zhou, B.-S. Shi, and G.-C. Guo, Nat. Commun. **7**, 13514 (2016).
- L.-M. Duan, M. D. Lukin, J. I. Cirac, and P. Zoller, Nature **414**, 413 (2001).
- M. D. Reid, Phys. Rev. A **40**, 913 (1989).
- M. D. Reid, P. D. Drummond, W. P. Bowen, E. G. Cavalcanti, P. K. Lam, H. A. Bachor, U. L. Andersen, and G. Leuchs, Rev. Mod. Phys. **81**, 1727 (2009).
- S. Mancini, V. Giovannetti, D. Vitali, and P. Tombesi, Phys. Rev. Lett. **88**, 120401 (2002).
- R. Chrapkiewicz, M. Dąbrowski, and W. Wasilewski, Preprint arXiv:1604.06049 (2016).
- P.-A. Moreau, J. Mougin-Sisini, F. Devaux, and E. Lantz, Phys. Rev. A **86**, 010101 (2012).
- M. Hosseini, B. M. Sparkes, G. Hétet, J. J. Longdell, P. K. Lam, and B. C. Buchler, Nature **461**, 241 (2009).
- D. Rieländer, K. Kutluer, P. M. Ledingham, M. Gündoğan, J. Fekete, M. Mazzeo, and H. de Riedmatten, Phys. Rev. Lett. **112**, 040504 (2014).
- A. Tiranov, J. Lavoie, A. Ferrier, P. Goldner, V. B. Verma, S. W. Nam, R. P. Mirin, A. E. Lita, F. Marsili, H. Herrmann, C. Silberhorn, N. Gisin, M. Afzelius, and F. Bussiès, Optica **2**, 279 (2015).
- C. Schaeff, R. Polster, M. Huber, S. Ramelow, and A. Zeilinger, Optica **2**, 523 (2015).
- S. Armstrong, M. Wang, R. Y. Teh, Q. Gong, Q. He, J. Janousek, H.-A. Bachor, M. D. Reid, and P. K. Lam, Nat. Phys. **11**, 167 (2015).
- K. Sun, J.-S. Xu, X.-J. Ye, Y.-C. Wu, J.-L. Chen, C.-F. Li, and G.-C. Guo, Phys. Rev. Lett. **113**, 140402 (2014).